Quantification of Tidal Asymmetry and Its Nonstationary Variations

Guo, Leicheng; Wang, Zhengbing ; Townend, Ian; He, Qing

DOI
10.1029/2018JC014372

Publication date
2019

Document Version
Final published version

Published in
Journal Of Geophysical Research-Oceans

JGR Oceans

RESEARCH ARTICLE
10.1029/2018JC014372

Key Points:
- Both harmonic and statistical methods are effective in indicating tidal asymmetry
- Statistical methods are applicable in quantifying nonstationary variations
- We find nonlinear effects of river discharge on tidal asymmetry in long estuaries

Supporting Information:
- Supporting Information S1

Correspondence to:
L. Guo,
lcguo@sklec.ecnu.edu.cn

Citation:
Guo, L., Wang, Z. B., Townend, I., & He, Q. (2019). Quantification of tidal asymmetry and its nonstationary variations. *Journal of Geophysical Research: Oceans*, *124*. https://doi.org/10.1029/2018JC014372

Received 15 JUL 2018
Accepted 2 JAN 2019
Accepted article online 5 JAN 2019

Quantification of Tidal Asymmetry and Its Nonstationary Variations

Leicheng Guo[1], Zheng Bing Wang[1,2,3], Ian Townend[1,4], and Qing He[1]

[1]State Key Lab of Estuarine and Coastal Research, East China Normal University, Shanghai, China, [2]Department of Hydraulic Engineering, Faculty of Civil Engineering and Geosciences, Delft University of Technology, Delft, Netherlands, [3]Marine and Coastal Systems Department, Deltares, Delft, Netherlands, [4]School of Ocean and Earth Sciences, University of Southampton, Southampton, UK

Abstract Tidal wave deformation and tidal asymmetry widely occur in tidal estuaries and lagoons. Tidal asymmetry has been intensively studied because of its controlling role on residual sediment transport and large-scale morphological evolution. There are several methods available to characterize tidal asymmetry prompting the need for an overview of their applicability and shortcomings. In this work we provide a brief review and evaluation of two methods, namely, the harmonic method and the statistical method. The latter comprises several statistical measures that estimate the probability density function and various forms of skewness. We find that both the harmonic and statistical methods are effective and have complementary advantages. The harmonic method is applicable to predominantly semidiurnal or diurnal regimes, while the statistical methods can be used in mixed tidal regimes. Assisted by harmonic data, a modified skewness measure can isolate the contribution of different tidal interactions on net tidal asymmetry and also reveal its subtidal variations. The application of the skewness measure to nonstationary river tides reveals stronger tidal asymmetry during spring tides than neap tides, and the nonlinear effects of river discharges on tidal asymmetry in the upper and lower regions of long estuaries.

Plain Language Summary Astronomical tide is the primary forcing that drives water motion and subsequent sediment transport and morphological changes in coastal and estuaries waters. Tidal waves propagating from open oceans into tidal estuaries and lagoons often experience changes in wave amplitude, speed, and shape, displaying tidal wave deformation and associated tidal asymmetry that is featured by unequal rising and falling tidal periods. This work first provides a brief review of the methods available for the quantification of tidal asymmetry in varying tidal environments, and discusses their applicability based on constructed data. The application of these two methods to measured nonstationary tides in a long estuary under significant time-varying river discharges reveal strongly nonlinear and nonuniform features of tidal asymmetry. The findings of this work have implications for the interpretation of high water levels in flood management and large-scale estuarine morphological evolution.

1. Introduction

Sediment transport is a focal point in coastal management, particularly in tidal estuaries and lagoons where there is conflicting interest between coastal developments and tidal wetland conservation under sea level rise. Other than the controlling impacts of sediment source availability, the dynamic processes leading to residual (tide-averaged) sediment transport are of significant relevance in examining erosion and deposition and consequent morphological changes (Dronkers, 1986). Tidal asymmetry is recognized as one of the most important processes in creating residual sediment transport and associated large-scale morphological changes in tidal environments including estuaries, tidal inlets and lagoon systems, and coastal waters (de Swart & Zimmerman, 2009). Tidal asymmetry in general refers to the phenomenon of tidal wave deformation (Pugh, 1987; Friedrichs & Aubrey, 1988). This leads to an unequal duration of the rise and fall of the height of the tide (vertical tide) and, consequently, offsets between the strength of the flood and ebb velocities (horizontal tide). Moreover, examination of tidal wave deformation and tidal asymmetry also deepens our understandings of tidal dynamics in shallow coastal waters and has implication as regards coastal flooding and management (Godin, 1985, 1999; Guo et al., 2015). Overall, tidal asymmetry has been well examined regarding its behavior and variability (Dronkers, 1986; Friedrichs & Aubrey, 1988; Wang et al., 1999) and its controlling effects on residual sediment transport and large-scale morphodynamics (Gatto et al., 2017; Guo, Song, et al., 2016; Guo, van der Wegen, et al., 2016; Postma, 1961).

In this work we discuss three types of tidal asymmetry: (1) unequal rising and falling tidal durations of vertical tides, called *tidal duration asymmetry*; (2) uneven peak ebb and flood velocities, called *peak current asymmetry*; and (3) unequal high water and low water slack durations in tidal currents, called *slack water asymmetry* (Dronkers, 1986; Gong et al., 2016; Guo et al., 2018). A shorter rising tide than falling tide, stronger peak flood currents than ebb currents, or a longer high water slack than low water slack result in flood dominance. Conversely, a shorter falling tide, stronger ebb currents, or longer low water slack promote ebb dominance. Flood dominance will cause flood-directed residual sediment transport, sediment import, and tidal basin infilling, while ebb dominance will cause seaward sediment flushing, sediment export, and tidal estuary emptying.

Tidal duration asymmetry has been more widely examined compared to peak current asymmetry, and slack water asymmetry because tidal water level data are readily more available than tidal currents. Tidal duration asymmetry and peak current asymmetry are coherently connected, such that a shorter rising tide will lead to stronger flood currents in the absence of significant river discharges. In addition, nontidal forcing such as river discharge and storm surges can profoundly modulate tidal propagation and deformation, thus altering tidal asymmetry as well. Storm surges affect tidal waves given their comparable space and time scales in shallow waters (LeBlond, 1991). River discharge is usually nonstationary and can raise mean water level (Cai et al., 2016), reduce tidal amplitudes, retard tidal phases (Godin, 1985, 1991), and enhances wave deformations (Guo et al., 2015) inside tidal estuaries. The duration of rising tides become shorter and falling tides become longer under a significant river discharge, suggesting enhanced tidal wave deformation. Moreover, nontidal forcing and/or hypsometric effects of intertidal flats may cause modification of tidal currents such that tidal duration asymmetry and peak current asymmetry may become inconsistent, that is, shorter rising tide coexists with stronger ebb currents in tidal estuaries with a significant river discharge (Friedrichs & Aubrey, 1988; Guo et al., 2014). These variations ask for more specific examinations of tidal asymmetry by different quantification methods.

A number of studies have examined the nature and variability of tidal asymmetry in varying tidal environments (Aubrey & Speer, 1985; Friedrichs & Aubrey, 1988; Guo et al., 2018; Nidzieko, 2010; Song et al., 2011; Speer & Aubrey, 1985; Wang et al., 1999, 2002). Different methods are used to characterize and quantify tidal asymmetry, but so far the applicability, advantages, and shortcomings of these methods have not been addressed. In this work we provide a review and evaluation of two methods available as hydraulic measures of tidal asymmetry, namely: (1) harmonic method, which is based on the phase differences and amplitude ratios of the interacting tidal constituents, and (2) a set of statistical measures that estimate probability density function (PDF) and various forms of skewness using tidal heights or tidal currents. Other than the hydraulic measures, there are morphological metrics which are used to characterize tidal asymmetry and residual sediment transport, that is, the proxy using tidal amplitude to water depth ratio and intertidal storage volume to channel volume ratio (Friedrichs & Aubrey, 1988), and an indicator based on relative change rates of high- and low-water surface area (Dronkers, 1986). These morphological metrics have recently been reviewed by Zhou et al. (2018) and link closely to the hydraulic measure examined in this work.

2. Data Used

We apply the methods to two types of data to provide a comprehensive evaluation of their applicability in varying environments. The first data are reconstructed tidal signals based on the harmonic constants of user-selected constituents, that is, the reconstructed signals based on $M_2 + M_4$ or $M_2 + O_1 + K_1$ constituents with different amplitudes and phases. These data sets are used to check the effectiveness of different methods when the nature of tidal asymmetry is straightforward to detect from the signals. Application and discussion of these data follow the descriptions of the methods in section 3.

The second type of data are actual tidal height measurements in the Changjiang River estuary in China that is used to demonstrate the advantages and shortcoming of the methods (Figure 1). The Changjiang River estuary is a meso-tidal coastal plain estuary physically forced by mixed tides with tidal ranges up to 5 m and a river discharges seasonally varying in the range of 10,000–60,000 m^3/s at Datong (the tidal wave limit) (Guo et al., 2015). Tidal wave propagation in the Changjiang River estuary is modulated by basin geometry, shallow water effects, and highly varying river discharges, thus exhibiting strong tidal wave deformation and nonstationary behaviors and associated spatial variability. For instance, strong tidal wave amplification and

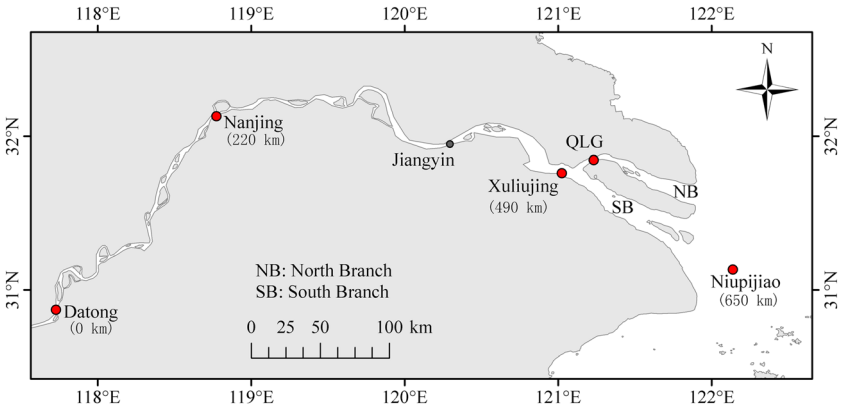

Figure 1. Sketch of the Changjiang River estuary and tidal gauges. The numbers in the brackets indicate the seaward distance to Datong, the tidal wave limit in the dry season. Niupijiao represents the river mouth, and Xuliujing and Nanjing represent the lower and upper estuaries, respectively, with the division roughly at Jiangyin (Guo et al., 2015). QLG is the abbreviation of Qinglonggang.

tidal bores take place in the landward portion of the North Branch, that is, at Qinglonggang (QLG; because of high convergence and the limited influence of river discharge; Figure 1), displaying a different behavior to the South Branch (see section 4.1). Moreover, we also collect one-year tidal height data (hourly interval) at 80 gauges along the U.S. coasts from websites of NOAA (https://co-ops.nos.noaa.gov) (see Figure S1). Only the gauges along the open coasts are selected (these inside estuaries and lagoons are omitted to avoid river influences). Furthermore, we will also include tidal current data which are from a numerical model of a short tidal estuary, the Newport Bay in Southern California (see section 3.2). More descriptions of the tidal data in the Changjiang River estuary and in Newport Bay can be found in Guo et al. (2015) and Guo et al. (2018), respectively, thus are not repeated here. Tidal harmonic analysis is then performed to the tidal height and tidal current data by using the T_Tide function (Pawlowicz et al., 2002), which outputs tidal harmonics (amplitudes and phases) for quantification of the tidal asymmetry.

3. Method Review

In this section we present two types of method, namely, the harmonic method and the statistical method. The harmonic method has been widely used in previous studies, and the occurrence of tidal asymmetry is evaluated based on the phase differences of the tidal constituents (resolved by harmonic analysis of tidal water levels or tidal currents) that interact and create tidal wave deformation (section 3.1). The statistical methods have several forms, including calculating the probability distribution function of tidal heights and (rising and falling) tidal durations (section 3.2), and evaluating the skewness of the time derivative of tidal water levels or the transformed skewness of tidal water levels (section 3.3). These statistical methods do not rely on harmonic analysis, but, instead, examine the statistical properties of tidal waves to infer wave deformation and consequent tidal asymmetry.

3.1. Harmonic Method

The harmonic method used to characterize tidal asymmetry is based on the tidal harmonics (amplitudes and phases of tidal constituents) resolved from actual tidal data. Two indicators are included, that is, the phase differences and amplitude ratios between two or more tidal constituents that interact and generate tidal asymmetry. As indicated in Song et al. (2013), the interacting tidal constituents satisfying a frequency relationship such as $2\omega_1 = \omega_2$, $3\omega_1 = \omega_2$, and $\omega_1 + \omega_2 = \omega_3$ (ω is the frequency; the subscript indicates different tidal constituents) can generate tidal asymmetry. Hence, the phase differences such as $2\theta_1$-θ_2, $3\theta_1$-θ_2, and $\theta_1 + \theta_2$-θ_3 (θ is phase) are used to indicate the nature of tidal asymmetry (Friedrichs & Aubrey, 1988; Song et al., 2013). For instance, the M_2-M_4 interactions ($2\omega_{M2} = \omega_{M4}$) are widely recognized as the dominant cause of tidal wave deformation and associated tidal asymmetry (Friedrichs & Aubrey, 1988; Speer & Aubrey, 1985). Therefore, a phase difference of $2\theta_{M2}$-θ_{M4} in the range of 0~180° leads to a shorter rising tide than falling tide thus flood dominance (Figure 2b), while a phase difference in the range of 180~360° leads to

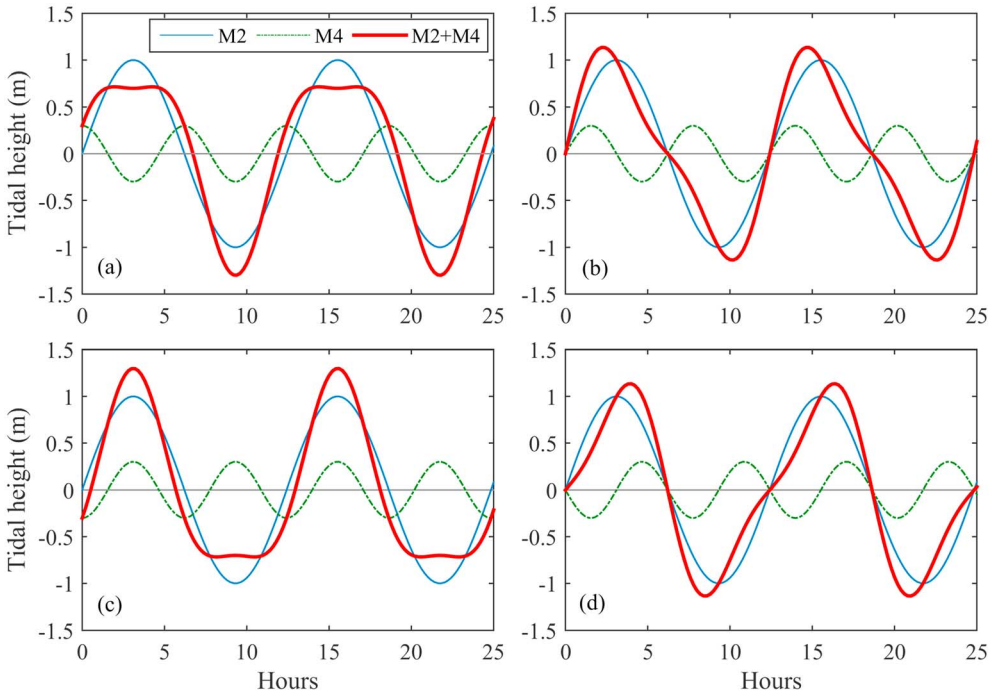

Figure 2. Tidal heights by M_2, M_4, and $M_2 + M_4$ tides with a phase difference $2\theta_{M2}$-θ_{M4} of (a) 0, (b) 90°, (c) 180°, and (d) 270°. The A_{M4}/A_{M2} amplitude ratio is 0.3.

a shorter falling tide and ebb dominance (Figure 2d). A $2\theta_{M2}$-θ_{M4} phase difference of exactly 0 or 180° will lead to equal rising and falling tides thus no tidal asymmetry, although the waveshape is statistically skewed (Figures 2a and 2c). Under the same phase difference, the A_{M4}/A_{M2} amplitude ratio (A is the tidal amplitude) is used to indicate the magnitude of the tidal asymmetry. A larger-amplitude ratio implies stronger tidal wave deformation and tidal asymmetry. Successful applications of the harmonic method to predominantly semidiurnal regimes, for example, U.S. Atlantic coasts (Friedrichs & Aubrey, 1988), Dutch coasts (Wang et al., 1999), and idealized tidal basins driven by M_2 tide only (Guo et al., 2014), have confirmed its effectiveness.

Similarly, the dual tidal interactions such as M_2-M_6 ($3\omega_{M2} = \omega_{M6}$) and K_1-K_2 ($2\omega_{K1} = \omega_{K2}$) can generate tidal asymmetry, and they can be quantified by phase differences such as $3\theta_{M2}$-θ_{M6} (Blanton et al., 2002) and $2\theta_{K1}$-θ_{K2} (Jewell et al., 2012), respectively. Moreover, triad tidal interactions such as M_2-M_4-M_6 ($\omega_{M2} + \omega_{M4} = \omega_{M6}$), M_2-S_2-MS_4, M_2-N_2-MN_4, M_2-O_1-K_1, and S_2-K_1-P_1 have been shown to generate measurable tidal asymmetry in tidal estuaries, and accordingly, the tidal asymmetry can be quantified by phase differences of $\theta_{M2} + \theta_{M4}$-$\theta_{M6}$, $\theta_{M2} + \theta_{S2}$-$\theta_{MS4}$, $\theta_{M2} + \theta_{N2}$-$\theta_{MN4}$, $\theta_{O1} + \theta_{K1}$-$\theta_{M2}$, and $\theta_{K1} + \theta_{P1}$-$\theta_{S2}$, respectively (van de Kreeke & Robaczewska, 1993; Hoitink et al., 2003; Song et al., 2011; Guo, Song, et al., 2016). A phase difference in the range of 0~180° will cause a shorter rising tide than falling tide and flood dominance, similar in the $2\theta_{M2}$-θ_{M4} case.

The harmonic method can be used to indicate peak current asymmetry in a similar way as tidal duration asymmetry based on the harmonics of resolved tidal currents. In short tidal basins with limited intertidal flats and insignificant river discharge where standing waves form, vertical tides and horizontal tides are in quadrature (Nidzieko, 2010). Therefore, a phase difference of tidal currents, for example, $2\Phi_{M2}$-Φ_{M4} or $\Phi_{O1} + \Phi_1$-Φ_{M2} (Φ is phase of horizontal tides), in the range of 90~270° indicates ebb dominance and that between −90° and 90° indicates flood dominance (Friedrichs & Aubrey, 1988; Guo et al., 2014, Guo, Song, et al., 2016). For instance, the phase differences of $\theta_{O1} + \theta_{K1}$-$\theta_{M2}$ and $\Phi_{O1} + \Phi_1$-Φ_{M2} are 253° and 181°, respectively, in Newport Bay, both indicating ebb dominance (Guo et al., 2018). It is understandable because a shorter falling tide than rising tide needs larger ebb currents to convey the same tidal prism; thus, ebb dominance takes place.

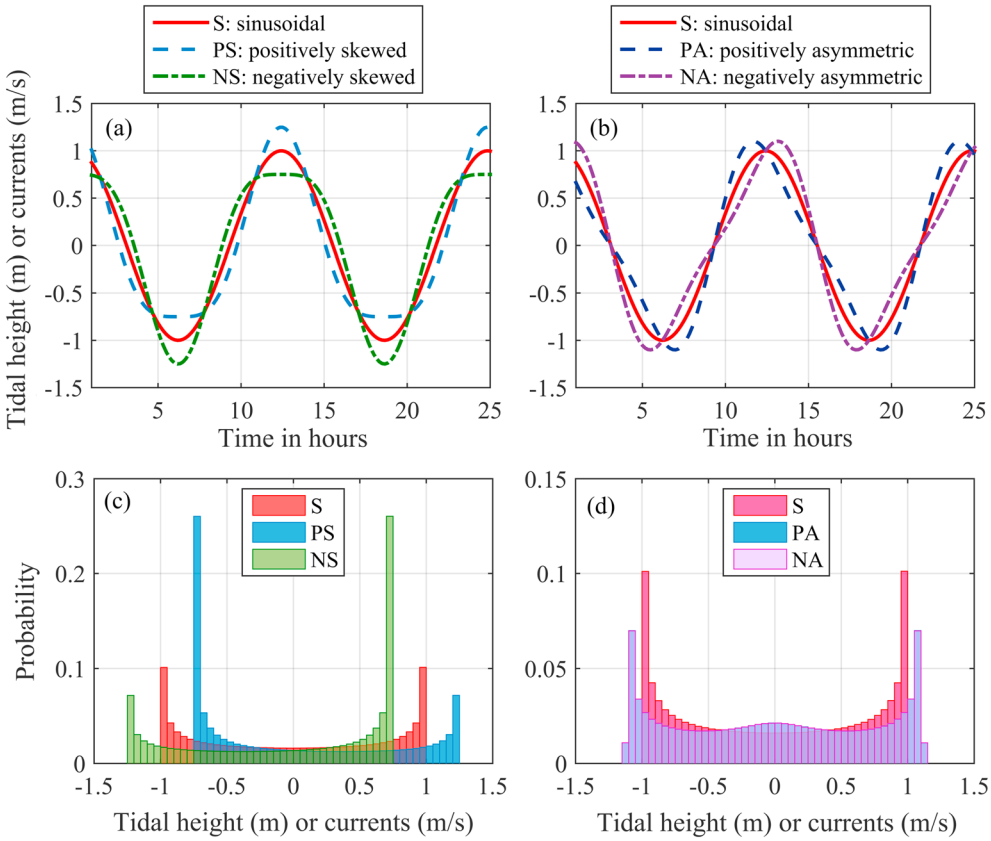

Figure 3. (a) Skewed and (b) asymmetric tidal wave or tidal current curves and (c and d) their corresponding PDFs. The positively and negatively asymmetric curves in (b) have the same PDF; thus, they are overlapped in (d). The flood currents are positive and ebb currents are negative in (a) and (b).

3.2. Statistical Method, Measure I—Probability Density Function

In addition to the harmonic method, tidal asymmetry has been characterized by statistical measures. One approach is to use the PDF of the time series of tidal heights (referenced to mean water level), referred to as the tidal height PDF, or TH-PDF. We see that a symmetric sinusoidal tidal signal has a bimodal distribution, for the TH-PDF. Deviation from this bimodal distribution suggests waveshape deformation although not necessarily tidal asymmetry (Ranasinghe & Pattiaratchi, 2000). For instance, the TH-PDFs of the constructed tidal signals (reconstructed based on M_2 and M_4 constituents as shown in Figure 2) with or without tidal asymmetry are similarly symmetric; thus, we cannot tell which one is flood or ebb dominant (Figure 3). To overcome that, Castanedo et al. (2007) reported a wave-by-wave method to characterize tidal statistics by estimating the PDFs of four variables, that is, the time series of wave crest (a) and trough (b) amplitudes, mean level (m), and standard deviation (s) of the tidal height. A sinusoidal wave without tidal asymmetry will have $a = b = \mathrm{A}$, $m = 0$, and $s = \sqrt{2}\mathrm{A}/2$. Based on a long time series of tidal height data, a scatterplot of the four variables against tidal height will exhibit deviations from their values for symmetric sinusoidal waves, thus possibly indicating tidal asymmetry. However, this wave-by-wave method only indicates the occurrence of tidal asymmetry but not its nature (flood or ebb dominance).

Another approach is based on the PDF measure of the time series of rising (indicated with a positive sign) and falling (indicated with a negative sign) tidal durations, referred to as the tidal duration PDF, or TD-PDF. The rising and falling tidal durations are directly derived from the tidal water level data. Statistical indicators of the TD-PDF are then used to quantify tidal duration asymmetry, that is, the skewness indicator (see section 3.3). In a simplified form, an equal percentage of rising and falling tidal durations indicates no tidal asymmetry, while food dominance occurs when the average rising tidal duration is <50% of the total period, and the converse is true for ebb dominance (Jewell et al., 2012; Lincoln & Fitzgerald, 1988). Such a definition

is consistent with the concept of tidal duration asymmetry, and it is theoretically applicable to all tidal regimes. Application of the TD-PDF to the constructed tidal signals (see Figure 2) suggests a percentage of rising tidal durations of 36% and 64% for the composite $M_2 + M_4$ tides in Figures 2b and 2d, respectively, suggesting flood dominance and ebb dominance that agrees with the harmonic method. Note that hourly tidal water level data are not enough to provide an accurate estimation of the falling and rising tidal durations; thus, long time series of data with a high time resolution are needed to accomplish significant differences between falling and rising tidal durations and to get rid of short-term periodic variability when the tidal signals are complex (see section 4.1).

The PDF measure also applies to the characterization of peak current asymmetry by examining the PDF of tidal currents, referred to here as tidal current PDF, or TC-PDF. To account for the nonlinear relationship between sediment transport and velocity, for example, an exponentially higher sediment transport capacity for larger current velocities, the TC-PDF is better estimated by using u^3 instead of u (u is the tidal current) (see Figure S2). Being similar to the TD-PDF, a larger percentage (>50%) of cubed flood currents than ebb currents, that is, a higher probability of the occurrence of flood currents, indicates flood dominance (Ranasinghe & Pattiaratchi, 2000). The TC-PDF is in essence similar to the skewness measure that considers a cubic numerator of currents (see equation (1) in section 3.3).

3.3. Statistical Method, Measure II—Skewness

3.3.1. Statistical Skewness

Skewness is a statistical measure of the asymmetry present in the PDF of an input signal compared to a normal distribution. The skewness measure characterizes the degree of asymmetry about the horizontal axis (up-and-down asymmetry) and the asymmetry measure represents the degree of asymmetry about the vertical axis (front-and-back asymmetry) of a PDF. The skewness indicator is calculated as follows:

$$Sk(x) = \frac{\frac{1}{N\text{-}1}\sum_{t=1}^{N}(\eta_t - \overline{\eta})^3}{\left[\frac{1}{N\text{-}1}\sum_{t=1}^{N}(\eta_t - \overline{\eta})^2\right]^{3/2}} \tag{1}$$

where Sk is the skewness indicator, η_t is the time series of the input signal, $\overline{\eta}$ is the mean value, and N is the length of equidistant time series data. The skewness method has been used in a wide variety of geophysical fields, such as for the characterization of turbulence nonlinearity in fluid mechanics and acoustic wave transformation (Reichman et al., 2016; Shepherd et al., 2011). A positive skewness of an input signal indicates a longer and/or flatter tail on the right side of its PDF (median value < mean value), and conversely, a negative skewness indicates a longer and/or flatter tail on the left side (median value > mean value).

When applying equation (1) to tidal water levels, we see that the skewness indicators are nonzero for both the positively and negatively skewed signals in Figure 3a (i.e., skewed TH-PDF), whereas the two signals actually have equal rising and falling tidal durations (i.e., no tidal asymmetry). Similarly, the skewness indicators are zero for both the positively and negatively asymmetric signals in Figure 3b (i.e., nonskewed TH-PDF), whereas the two signals are actually featured by unequal rising and falling durations (i.e., with tidal asymmetry). It thus implies that using the tidal water levels as input signals in equation (1) cannot indicate tidal asymmetry, and some modifications of this method are outlined the following sections.

3.3.2. Transformed Skewness

One solution is to use an asymmetry proxy, a transformed skewness measure. It is a skewness measure of the imaginary part of a Hilbert-transformed input signal. It reads as

$$As = Sk\{imag[H(\eta)]\} \tag{2}$$

where As is the transformed skewness measure, $H(\cdot)$ indicates the Hilbert transform, and $imag(\cdot)$ indicates the imaginary part (the real part of the output of a Hilbert transform is the input signal itself). The transformed skewness measure has been used in characterizing wave-induced current asymmetry under short-wave impacts (Ruessink et al., 2009). For a time series of tidal water levels, the imaginary part of a Hilbert-transformed tidal height leads to positive and negative outputs for falling and rising tides, respectively (see Figure S3). Therefore, a positive value of the transformed skewness measure suggests longer

rising tidal durations than falling tide durations on average (i.e., ebb dominance), and a negative value indicates longer falling tidal durations (i.e., flood dominance) (Bruder et al., 2014). To further validate the general effectiveness of the transformed skewness, we apply it to the constructed signals in Figure 3 and find that the transformed skewness is consistently zero for the sinusoidal signal (S), and the positively (PS) and negatively (NS) skewed signals in Figure 3a, thus implying no tidal asymmetry. The transformed skewness is −0.48 and 0.48 for the positively (PA) and negatively (NA) asymmetric signals in Figure 3b, suggesting longer falling and rising tidal durations, respectively. The evaluation by the transformed skewness measure is therefore consistent with the harmonic method, demonstrating its effectiveness as a suitable measure of tidal asymmetry.

3.3.3. Derivative Skewness

Another option of is to use the time derivatives of tidal height as the input signal in equation (1) instead of tidal height itself (Nidzieko, 2010), called derivative skewness, as follows:

$$Sk_{TDA} = Sk(d\eta/dt) \tag{3}$$

where TDA stands for tidal duration asymmetry. The time derivative ($d\eta/dt$) transforms rising and falling tidal water levels into positive and negative gradients (see Figure S3), thus enabling tidal duration asymmetry estimation in a similar way to the Hilbert transform in equation (2). A positive derivative skewness indicates a shorter rising tide than falling tide and flood dominance, while a negative derivative skewness demonstrates a shorter falling tide and ebb dominance. Applying the derivative skewness measure to the constructed signals will give zero value for signals S, PS, and NS in Figure 3a, but 0.76 and −0.76 for signals PA and NA, respectively, in Figure 3b, implying its applicability. Note that the transformed and derivative skewness measures have opposite sign for the same tidal asymmetry. The derivative skewness method was further extended and used to isolate the contribution of tidal interactions like M_2-M_4, M_2-O_1-K_1, and S_2-K_1-P_1 on the total tidal asymmetry (Song et al., 2011), and to uncover fortnightly variations of tidal duration asymmetry when applying equation (3) using a moving window (e.g., three days) (Guo, van der Wegen, et al., 2016).

When applying the transformed skewness (equation (2)) and derivative skewness (equation (3)) measures in their present form, we find that the cubic numerator in the skewness indicator (in equation (1)) will amplify the rising and falling rates of tidal height and this nonlinear amplification may cause misleading results. Preliminary test of the derivative skewness method on artificially generated signals (with fixed falling and rising tidal duration but different rising and falling limbs) suggested that the derivative skewness varies in a considerable range, that is, −0.1~1.2, and can be even negative when the rising tide is actually shorter than falling tide (see Figure S4). A similar discrepancy also occurs for the transformed skewness given by equation (2) (see Figure S4). The discrepancies occur because the cubic numerator in equation (1) will significantly increase the statistical importance of large derivatives (e.g., large tidal height rising and falling rates). With respect to the shape of a PDF, the statistical skewness does not distinguish the impacts of a long or a flat tail; therefore, zero skewness may indicate a symmetric PDF or an asymmetric PDF with a long tail and a flat tail on either side when the asymmetry evens out. To overcome this, Guo et al. (2018) suggested an improvement by employing the derivative skewness to the time series of high water (HW) and low water (LW); thus, the nonlinear variations in the rising and falling limbs of the tidal water level curves are removed and only the duration differences between HW-LW or LW-HW will affect the skewness measure. The calculation then reads as follows:

$$Sk_{\mathrm{TDA}} = Sk(d\eta_{\mathrm{HW-LW}}/dt) \tag{4}$$

where $\eta_{\mathrm{HW\text{-}LW}}$ indicates the filtered time series signals with HW and LW only (with linear interpolation between HW and LW to obtain equidistance data if necessary). The same HW-LW series of data can be also used as input to the transformed skewness measure. Preliminary application of the filtered derivative skewness has demonstrated its effectiveness to accurately indicate tidal duration asymmetry (Guo et al., 2018). When applying both equations (3) and (4) to the tidal height data collected along the U.S. coasts, we see that the derivative skewness of the original (unfiltered data) is overall larger in magnitude that of the filtered data (see Figure S5). It suggests that using the time series of HW-LW (equation (4)) may underestimate the tidal asymmetry.

3.3.4. Skewness Measure Applied to Tidal Currents

The skewness measure is also applicable for quantification of peak current asymmetry and slack water asymmetry (Bruder et al., 2014; Gong et al., 2016; Guo et al., 2018). Skewed current curves (preponderance of large crests or troughs) have unequal peak ebb and flood currents, demonstrating the presence of peak current asymmetry but not slack water asymmetry (see Figure 3a). Similarly, asymmetric current curves have equal peak currents but uneven slack waters, thus indicating the presence of slack water asymmetry but not peak current asymmetry (see Figure 3b). The asymmetric current curves can be seen as acceleration-skewed; thus, it is in line with the definition of slack water asymmetry. To use the skewness measure for quantification of peak current asymmetry (PCA), the input signal is tidal currents:

$$Sk_{\mathrm{PCA}} = Sk(u) \qquad |u|>u_c \tag{5}$$

and for quantification of slack water asymmetry (SWA), the input signal is the acceleration of the currents:

$$Sk_{\mathrm{SWA}} = Sk(du/dt) \qquad |u|<u_c \tag{6}$$

where u is a time series of tidal currents and u_c is a velocity threshold to filter the tidal currents needed for transport of coarse sediments and for settling of fine sediments (Guo et al., 2018). Considering that sediment transport is a power function of velocity by an order of 3–5 (van Rijn, 1993), the skewness measure might be expected to a good measure for quantifying the peak current asymmetry because the cubic numerator in equation (1) emphasizes the sediment transport capacity of higher (both ebb and flood) current velocities. Hence, it can be taken to be an effective sediment-related tidal asymmetry indicator. When assuming that flood currents are positive, a positive PCA skewness indicates stronger flood currents and flood dominance, and a positive SWA skewness indicates shorter low-water slack and flood dominance as well. When taking the signals in Figure 3 as tidal currents (and assuming $u_c = 0.2$ m/s), the PCA skewness of S, PS, and NS signals (see Figure 3a) is 0, +0.49 (flood dominance), and −0.49 (ebb dominance), respectively, and the SWA skewness of S, PA, and NA signals (see Figure 3b) is 0, +1.33 (flood dominance), and −1.33 (ebb dominance), respectively. Gong et al. (2016) and Guo et al. (2018) had applied the skewness method (equation (6)) to indicate slack water asymmetry in estuaries. These results demonstrate that the skewness measures (equations (5) and (6)) can indicate the peak current asymmetry and slack water asymmetry.

4. Applications and Evaluation

4.1. Application to Actual Data

So far we see that both the harmonic and statistical methods are effective in indicating tidal asymmetry under constructed data. To further elaborate their applicability and their advantages and shortcomings, we apply these methods to actual tidal data obtained in the Changjiang River estuary. The tides in the Changjiang River estuary are dynamically highly nonlinear and nonstationary (Guo et al., 2015); hence, a single method is not able to characterize all tidal features and associated variations (Matte et al., 2013). For simplicity, the harmonic method, the PDF measure, and the filtered derivative skewness measure are applied and evaluated. The transformed skewness measure works in a similar way as the derivative skewness; thus, it is not discussed.

One year of tidal height data at three tidal gauges in the upper estuary, lower estuary, and estuary mouth are used to indicate along-river changes (see Figure 1). Harmonic analysis suggests that the Changjiang River estuary has a mixed tidal regime with an $(A_{O1} + A_{K1} + A_{P1})/(A_{M2} + A_{S2} + A_{N2})$ amplitude ratio of 0.24 at the mouth (Guo et al., 2015). M_2 is the largest constituent, followed by S_2, K_1, O_1, N_2, etc. Overtide and compound tides such as M_4 and MS_4 are small outside the estuary but become considerable inside the estuary (Guo et al., 2015). Past studies have shown that any combination of more than two constituents (both principal and higher and lower frequency harmonics) satisfying frequency relationships such as $2\omega_i = \omega_j$, $\omega_i + \omega_j = \omega_k$, and $\omega_i + \omega_j + \omega_k = \omega_s$ can create tidal asymmetry, that is, M_2-M_4, M_2-O_1-K_1, and M_2-S_2-N_2-MSN_2 interactions (Le Provost, 1991; Song et al., 2011). Therefore, tidal wave deformation and tidal asymmetry inside the Changjiang River estuary can be induced by M_2-M_4, M_2-O_1-K_1, M_2-S_2-MS_4, and M_2-N_2-MN_4 interactions (Guo et al., 2015). The $2\theta_{M2}$-θ_{M4} phase difference is ~70° and varies little along the estuary, suggesting flood dominance if considering M_2-M_4

interactions only. The harmonic analysis results show that the phase differences of $2\theta_{M2}$-θ_{M4}, $\theta_{M2} + \theta_{S2}$-$\theta_{MS4}$, and $\theta_{M2} + \theta_{N2}$-$\theta_{MN4}$ are nearly the same, and the $\theta_{O1} + \theta_{K1}$-$\theta_{M2}$ phase difference varies between 0 and 50° along the estuary (Guo, Song, et al., 2016). It implies that all of these tidal interactions will cause flood dominance. This result is in line with a shorter rising tide than falling tide (see next paragraph). But it remains unknown which interaction plays a bigger role in dominating the flood dominance. Note that the flood dominance here refers to tidal water levels but not tidal currents (the ebb currents are always stronger than flood currents because of significant river discharges). The nonstationarity in the tidal signals induced by river discharge imposes a challenge to resolve tidal harmonics precisely, particularly in the upper estuary where nonstationary river influences are strong (Guo et al., 2015).

Strong tidal wave deformation and formation of tidal bores in the North Branch of the Changjiang River estuary induce another difficulty for the harmonic method. The tidal waves are much more deformed on spring tides than neap tides in the North Branch, and tidal bores can be generated. The rising tides become much shorter while the falling tides are prolonged under the occurrence of tidal bores (suggesting flood dominance). These variations induce nonstationary behavior of tidal asymmetry. Moreover, the high water may persist as long as 2.5 hr while the change from falling to rising tide is sharp (see Figure S6). These peculiar features pose a challenge for conventional harmonic analysis. With 38 tidal constituents resolved at QLG (see Figure 1), the harmonic methods show an identical phase difference of $2\theta_{M2}$-θ_{M4}, $\theta_{M2} + \theta_{S2}$-$\theta_{MS4}$, and $\theta_{M2} + \theta_{N2}$-$\theta_{MN4}$ of ~82° (suggesting flood dominance) but the phase difference of $\theta_{O1} + \theta_{K1}$-$\theta_{M2}$ is ~350° (suggesting ebb dominance). It is thus not possible to tell the nature of the net tidal asymmetry based on the harmonic method alone. Moreover, comparison of the reconstructed signals based on the resolved harmonic constants with the measured tidal heights shows that the harmonic analysis cannot capture the flat high tide and sharp transition from falling to rising tide, leading to considerable discrepancies in the estimation of rising and falling tidal periods (see Figure S6).

Estimation of the average falling and rising tidal durations based on one-year tidal height data suggests that the mean falling tide duration is slightly longer (~0.03 hr) than rising tide at the estuary mouth and the duration inequality increases in the landward direction (e.g., falling tide is on average ~2.0 hr longer than rising tide in the upper estuary), reflecting a more distorted tidal wave in the inner estuary, owing to the combined impacts of friction, estuarine geometry, and river discharge. The PDFs of tidal heights show upstream tidal damping but not tidal asymmetry (Figures 4a–4c), while the PDFs of falling and rising tidal durations confirm the observation that falling tides become increasingly longer in the landward direction (Figures 4d–4f).

Application of the filtered derivative skewness method to the nonstationary river tides in the Changjiang River estuary reveals strong subtidal variations of tidal ranges and tidal duration asymmetry (Figures 5b and 5c) and associated nonuniform changes in response to high and low river discharges (Figures 5d and 5e). The mean water level and lower low tide are observed higher at spring tide than neap tide, in particular in the upper estuary (Guo et al., 2015; LeBlond, 1991; Sassi & Hoitink, 2013). To remove the influences of mean water levels, high-pass-filtered data are used for the derivative skewness measure. The derivative skewness for one-year data is 0.13, 1.37, and 2.32 at the mouth, in the lower, and upper estuary, respectively, suggesting overall shorter rising tides than falling tides throughout the estuary. Larger derivative skewness in the upper estuary suggests enhanced tidal wave deformation in the landward regions, particularly in the dry seasons when the river discharge is significant but not too large (Figures 5b and 5c). At fortnightly time scales, the derivative skewness is larger during spring tide than neap tide in both upper and lower estuaries, suggesting stronger wave deformation and tidal asymmetry during spring tides (Figure 5d). At seasonal time scales, the derivative skewness decreases with increasing river discharges in the upper estuary but increases in the lower estuary (Figure 5e). It suggests that tidal duration asymmetry is stronger under high river discharge in the lower estuary while it is smaller in the upper estuary. This result is consistent with decreasing A_{D4}/A_{D2} ratios (the amplitude ratio of quarter-diurnal to semidiurnal species) in the upper estuary and increasing ratios in the lower estuary with increasing river discharges in Guo et al. (2015). Analyses from a tidal energy perspective also confirm the above finding. Work by Zhang et al. (2016) suggests that the tidal asymmetry is one of the degrees of freedom used by the estuary to maintain a state of minimum work by adjusting tidal wave deformation and tidal asymmetry along the estuary under varying river discharges.

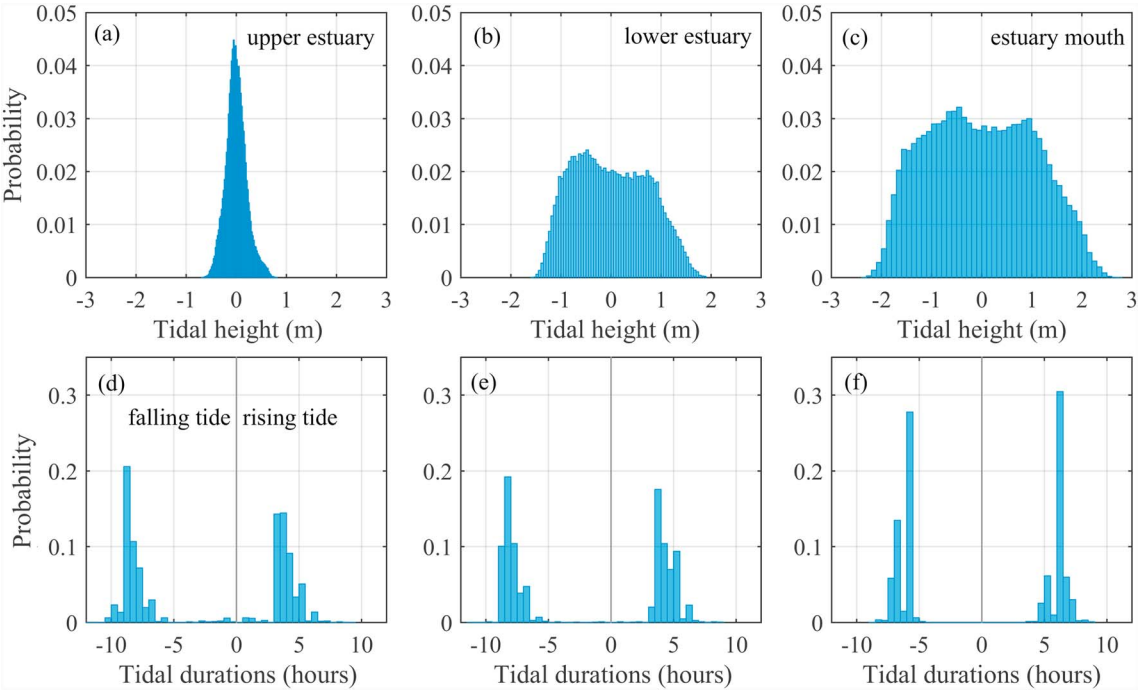

Figure 4. The (a–c) TH-PDFs of tidal heights and (d–f) TD-PDFs at stations in the upper estuary (landward regions, Nanjing in Figure 1) (a and d), lower estuary (seaward regions, Xuliujing) (b and e), and estuary mouth (Niupijiao) (c and f) based on two-year data (2009–2010) in the Changjiang River estuary. The tidal heights are referenced to local mean water level. Rising tidal duration is positive and falling tidal duration is negative.

The nonuniform behaviors of tidal wave deformation between upper (landward) and lower (seaward) regions of long tidal estuaries with significant river influence are not unique to the Changjiang River estuary. Godin (1985, 1999) reported that a larger river discharge will cause accelerated low water and retarded high water in the upper St. Lawrence Estuary, whereas it will hasten the progress of high water and delay low water in the lower estuary. Similar nonuniform changes also occur in the Amazon Estuary (Gallo & Vinzon, 2005). Model results also reveal nonlinear variations of tidal asymmetry in response to increasing river discharges (Guo, Song, et al., 2016). These findings do not violate our intuitional understanding of the impacts of river discharge in causing more tidal damping and wave distortion (throughout an estuary) because both low and high river discharges will prolong falling tides and shorten rising tides compared to the situation with zero river discharge.

The variations of the A_{D4}/A_{D2} amplitude ratios in response to increasing river discharge in Guo et al. (2015) are consistent with the derivative skewness variations in this work, and it may imply that the M_2-M_4 interaction is the dominant contribution to net tidal duration asymmetry. Based on tidal harmonics and the decomposition method suggested by Song et al. (2011), we estimate that the summed skewness of the four major interactions, that is, M_2-M_4, M_2-O_1-K_1, M_2-S_2-MS_4, and M_2-N_2-MN_4, is 0.17 and 1.11, at the mouth and in the lower estuary, respectively. They are in good agreement with the derivative skewness (0.13 and 1.37, respectively) obtained from tidal height data. We see that the M_2-M_4 interaction is indeed the major contribution to the net tidal asymmetry, with a contribution >45% in the lower estuary, followed by M_2-S_2-MS_4 (30%) and M_2-N_2-MN_4 (5%) interactions. The M_2-O_1-K_1 interaction is of relatively minor importance (<1%) because of smaller O_1 and K_1 amplitudes compared to M_2 and S_2. Similarly, we quantify that the derivative skewness of tidal height is 2.32 at QLG in the North Branch, and the contribution of M_2-M_4 interaction is 47% and that of M_2-O_1-K_1 interaction is −2% (negative value indicates an effect causing ebb dominance).

Quantification of peak current asymmetry under the influence of river discharges needs separate consideration. River discharge induces a seaward mean current (i.e., $-u_o$; the negative sign indicates seaward) and enlarges ebb currents, causing overall ebb dominance, although the rising tides are shorter than the falling tides. Even though, we find that the tide-related oscillatory currents (i.e., $\sum u_i \cos(\omega_i t + \theta_i)$; the subscript i

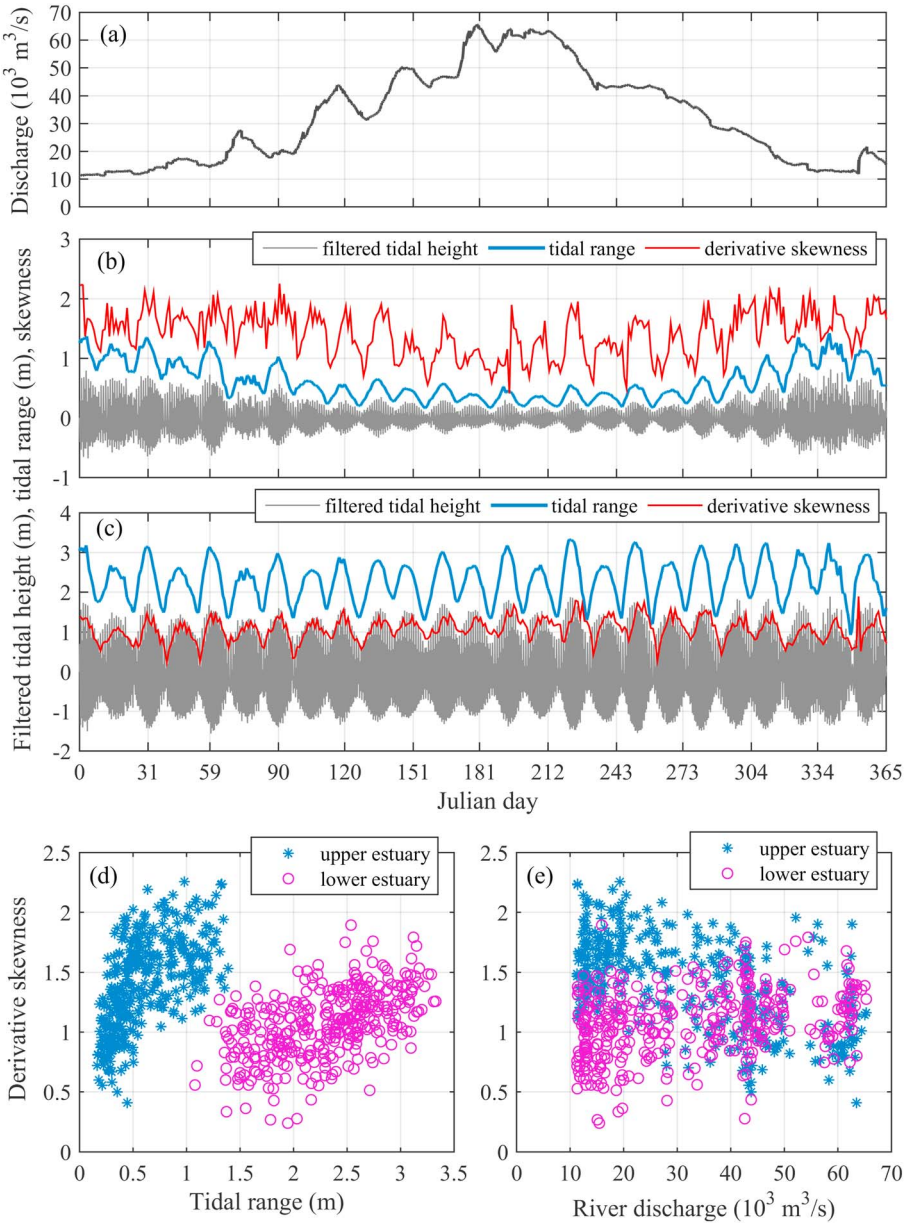

Figure 5. (a) River discharge at Datong in calendar year 2010; high-passed-filtered tidal height, tidal ranges, and filtered derivative skewness in the (b) upper estuary (Nanjing; see Figure 1) and (c) lower estuary (Xuliujing); (d) derivative skewness versus tidal range; and (e) derivative skewness versus river discharge in the Changjiang River estuary.

indicates the name of the tidal constituent), that is, the high-pass-filtered currents with the mean current removed, are still stronger in the flood direction than the ebb direction. For instance, with one year of tidal current data at Xuliujing in the Changjiang River estuary (Guo et al., 2015), we find that the high-pass-filtered currents have a positive PCA skewness of 0.03 based on equation (5) (assuming that flood currents are positive), suggesting stronger flood tidal currents and flood dominance. It is also validated by a $2\Phi_{M2}$-Φ_{M4} phase difference of ~25° (in the range of −90~90°, thus indicating flood dominance). Modeled tidal currents in a schematized estuary have also confirmed flood dominance of tide-induced oscillatory currents, although the ebb currents are stronger than flood currents due to river discharge (Guo et al., 2014). Note that it is the asymmetry in the total currents (i.e., $-u_o + \sum u_i \cos(\omega_i t + \theta_i)$) that controls the net residual sediment transport, although the contribution of river and tide-related asymmetry and river-tide interaction can be decomposed (Guo, Song, et al., 2014; Guo, Song, et al., 2016).

Table 1
A Summary of the Methods Available for Quantification of Tidal Asymmetry and Their Applicability and Criterions in Indicating Flood or Ebb Dominance

		Statistical Methods		
	Harmonic Method	PDF	Derivative Skewness	Transformed Skewness
Tidal duration asymmetry	Phase differences, that is, $2\theta_{M2}$-θ_{M4} and $\theta_{O1} + \theta_{K1}$-$\theta_{M2}$; phase differences in the range of 0~180° indicate flood dominance and that in the range of 180~360 ° indicate ebb dominance	TD-PDF of rising and falling durations, an average rising tidal duration > or <falling duration indicate ebb or flood dominance	Skewness of time derivative of the time series of HW and LW, a derivative skewness > or <0 indicates flood or ebb dominance, respectively	Skewness of the imaginary part of Hilbert-transformed tidal water levels, a transformed skewness > or <0 indicates ebb or flood dominance, respectively
Peak current asymmetry	Phase differences, that is, $2\Phi_{M2}$-Φ_{M4}; phase differences in the range of 90~270° indicate ebb dominance and that in the range of −90~90 ° indicate flood dominance	TC-PDF of the cubed ebb and flood currents, a percentage of cubed flood currents > or <cubed ebb currents indicate flood or ebb dominance	Skewness of tidal currents, a skewness > or <0 indicates flood or ebb dominance, respectively (assuming that flood currents are positive)	Not applicable
Slack water asymmetry	Not applicable	Applicable but has not been used	Skewness of tidal current accelerations, a skewness > or <0 indicates flood or ebb dominance, respectively (assuming that flood currents are positive)	

Note. θ and Φ indicate the phase of vertical and horizontal tidal components, respectively. A and U are the amplitudes of vertical and horizontal tides, respectively.

4.2. Advantages and Shortcomings of the Methods

The abovementioned applications and discussions suggest that both the harmonic method and the statistical methods are effective in indicating and quantifying tidal asymmetry, although their applicability differs slightly (Table 1). The advantages of the harmonic method include (1) having a solid physical background and being applicable to a large proportion of estuaries worldwide, where M_2 is the most important principal constituent; (2) easy to use because of the availability of harmonic constituent data for many locations; and (3) the impacts of nontidal forcing are accounted for by altered tidal amplitudes and phases. Its shortcoming lies in its inability to characterize net tidal asymmetry in mixed tidal regimes where multiple tidal interactions may either augment or cancel each other in creating tidal asymmetry, as that has been identified by Jewell et al. (2012).

On the other hand, we see that the derivative and transformed skewness measures have advantages in terms of their ability to (1) cope with complex tidal signals in semidiurnal, diurnal, or mixed tidal regimes; (2) indicate net asymmetry caused by multiple interactions and the separated contribution of individual interaction; (3) reveal subtidal variations; and (4) quantify both tidal duration asymmetry and peak current asymmetry. A weakness of the skewness method is the lack of strong physical foundation. The sign of the derivative and transformed skewness measures indicates the ebb or flood nature of tidal asymmetry while its absolute value only indicates the strength of tidal asymmetry in a relative manner. A physical understanding of the connections between tidal wave deformation and the skewness proxy has yet to be fully investigated.

Overall we see that the harmonic, statistical PDF, and skewness methods have complementary advantages and are best used in combination. When plotting the derivative skewness against the amplitude ratio (using the constructed signals consisting of $M_2 + M_4$ and $M_2 + O_1 + K_1$ constituents with different amplitude ratios and phase differences), we clearly see that the derivative skewness is zero for phase differences of 0 and 180° while it is maximal for phase differences of 90° and 270° regarding both M_2-M_4 and M_2-O_1-K_1 interactions (Figure 6). The tidal asymmetry induced by M_2-M_4 interaction tends to be strongest when the A_{M4}/A_{M2} ratio is 0.3–0.5 with a phase difference $2\theta_{M2}$-θ_{M4} of 90° or 270° (Figure 6a). We also see that the derivative skewness is overall larger for the M_2-M_4 interaction (Figure 6a) than the M_2-O_1-K_1 interaction (Figure 6b), suggesting possibly stronger effects of M_2-M_4 interaction in causing tidal asymmetry. These analyses suggest

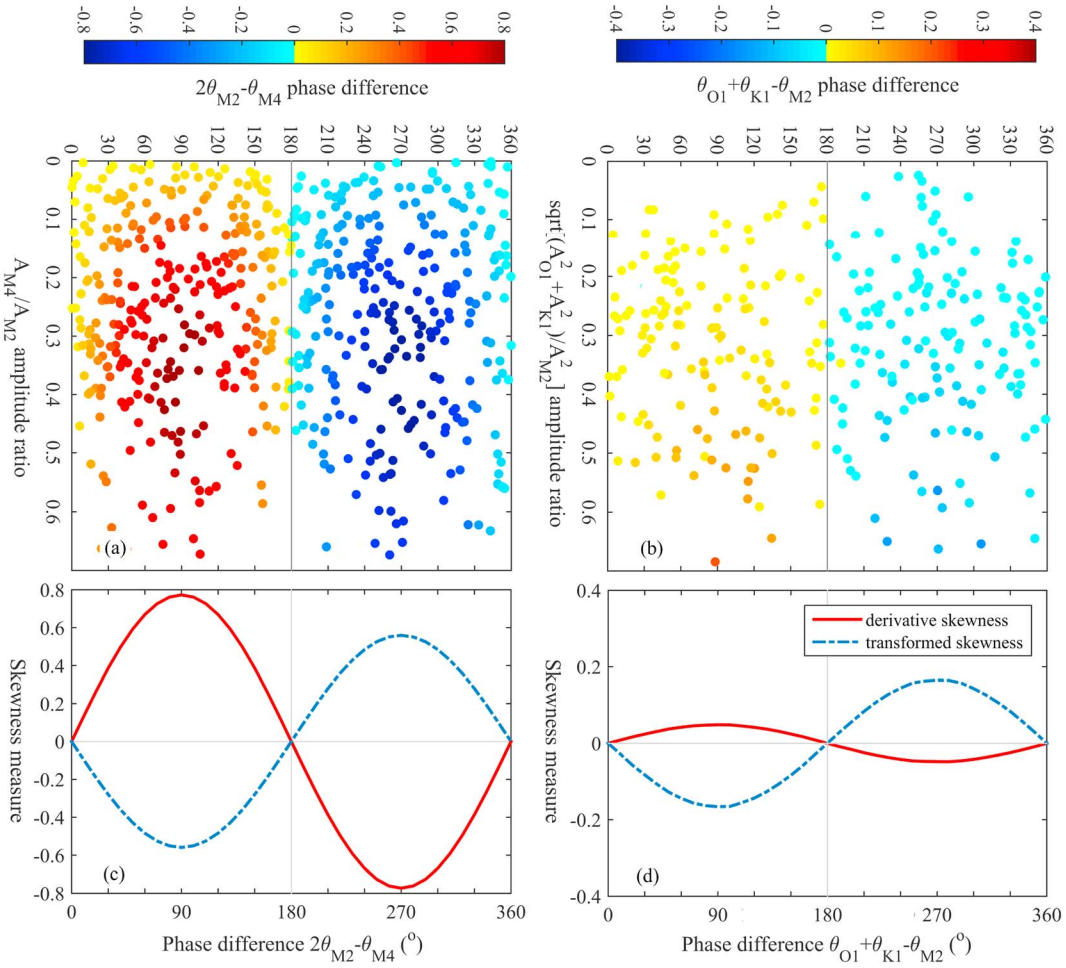

Figure 6. Scatterplot of filtered derivative skewness of tidal duration asymmetry due to (a) M_2-M_4 and (b) M_2-O_1-K_1 interactions for ideally constructed signals with different phase differences and amplitude ratios and (c and d) variations of derivative skewness and transformed skewness for an amplitude ratio of 0.3 but different phase differences. Positive derivative skewness and negative transformed skewness suggest flood dominance.

that the evaluations by the harmonic method and the skewness measures can be used interchangeably. Regarding their applicability, the harmonic method is preferred in predominantly semidiurnal or diurnal tidal regimes where single tidal interaction such as M_2-M_4 or M_2-O_1-K_1 controls the tidal asymmetry. The statistical PDF and skewness methods are the alternative options and have advantages in mixed tidal regime where multiple tidal interactions occur.

5. Conclusions

In this work we provide a brief review of two methods, that is, the harmonic and statistical methods, available for quantification of tidal asymmetry and find that they have complementary advantages. By estimating phase differences and amplitude ratios, the harmonic method has a well-defined physical foundation and is applicable to semidiurnal or diurnal tidal regimes. The statistics of the PDF of rising and falling tidal periods can be used to indicate tidal duration asymmetry and that of cubed tidal currents to indicate peak current asymmetry. We consider several forms of skewness measure and conclude that a filtered derivative skewness has better explanatory power. The skewness measure is applicable for all tidal environments and in particular for mixed tidal regimes. The skewness measure is able to reveal subtidal variations of tidal asymmetry and the relative contribution of different tidal interactions under mixed regimes. The harmonic and statistical skewness methods are not mutually exclusive but can be qualitatively linked.

Using the skewness measure, we find that the M_2-M_4 interaction induces much stronger tidal asymmetry even with small M_4 amplitude compared to other tidal interactions. We confirm that tidal asymmetry is stronger during spring tide than neap tide, and it exhibits distinctive behaviors in response to low and high river discharges between the upper and lower regions of long estuaries. We see that slack water asymmetry is relatively poorly studied compared to peak current asymmetry, and more work is needed regarding its controlling effect on residual fine sediment transport.

Acknowledgments
This work is supported by the project "Coping with deltas in transition" within the Programme of Strategic Scientific Alliance between China and The Netherlands (PSA), financed by the Ministry of Science and Technology of People's Republic of China (2016YFE0133700) and Royal Netherlands Academy of Arts and Sciences (KNAW) (PSA-SA-E-02), and also by National Natural Science Foundation of China (51320105005, 51739005, 41506105, 41876091), and Shanghai Committee of Science and Technology (17DZ1204800). We thank the two anonymous reviewers for their constructive comments.

References

Aubrey, D. G., & Speer, P. E. (1985). A study of non-linear tidal propagation in shallow inlet/estuarine systems. Part I: Observations. *Estuarine, Coastal and Shelf Science*, *21*(2), 185–205. https://doi.org/10.1016/0272-7714(85)90096-4

Blanton, J. O., Lin, G., & Elston, S. A. (2002). Tidal current asymmetry in shallow estuaries and tidal creeks. *Continental Shelf Research*, *22*(11-13), 1731–1743. https://doi.org/10.1016/S0278-4343(02)00035-3

Bruder, B., Bomminayuni, S., Hass, K., & Stoesser, T. (2014). Modeling tidal distortion in the Ogeechee estuary. *Ocean Model*, *82*, 60–69. https://doi.org/10.1016/j.ocemod.2014.08.004

Cai, H. Y., Savenije, H. H. G., Jiang, C. J., Zhao, L. L., & Yang, Q. S. (2016). Analytical approach for determining the mean water level profile in an estuary with substantial freshwater discharge. *Hydrology Earth System Science*, *20*(3), 1177–1195. https://doi.org/10.5194/hess-20-1177-2016

Castanedo, S., Mendez, F. J., Medina, R., & Abascal, A. J. (2007). Long-term tidal level distribution using a wave-by-wave approach. *Advances in Water Resources*, *30*(11), 2271–2282. https://doi.org/10.1016/j.advwatres.2007.05.005

de Swart, H. E., & Zimmerman, J. T. F. (2009). Morphodynamics of tidal inlet systems. *Annual Review of Fluid Mechanics*, *41*(1), 203–229. https://doi.org/10.1146/annurev.fluid.010908.165159

Dronkers, J. (1986). Tidal asymmetry and estuarine morphology. *Netherlands Journal of Sea Research*, *20*(2/3), 107–131.

Friedrichs, C. T., & Aubrey, D. G. (1988). Non-linear tidal distortion in shallow well-mixed estuaries: A synthesis. *Estuarine, Coastal and Shelf Science*, *27*(5), 521–545. https://doi.org/10.1016/0272-7714(88)90082-0

Gallo, M. N., & Vinzon, S. B. (2005). Generation of overtides and compound tides in the Amazon estuary. *Ocean Dynamics*, *55*(5-6), 441–448 . https://doi.org/10.1007/s10236-005-0003-8

Gatto, V. M., van Prooijen, B. C., & Wang, Z. B. (2017). Net sediment transport in tidal basins: Quantifying the tidal barotropic mechanisms in a unified framework. *Ocean Dynamics*, *67*, 1385–1406. https://doi.org/10.1007/s10236-017-1099-3

Godin, G. (1985). Modification of river tides by the discharge. *Journal of Waterway, Port, Coastal and Ocean Engineering*, *111*(2), 257–274. https://doi.org/10.1061/(ASCE)0733-950X(1985)111:2(257)

Godin, G. (1991). Frictional effects in river tides. In B. B. Parker (Ed.), *Tidal Hydrodynamics* (pp. 379–402). Toronto: John Wiley.

Godin, G. (1999). The propagation of tides up rivers with special consideration of the upper Saint Lawrence River. *Estuarine, Coastal and Shelf Science*, *48*, 307–324.

Gong, W. P., Schuttelaars, H., & Zhang, H. (2016). Tidal asymmetry in a funnel-shaped estuary with mixed semidiurnal tides. *Ocean Dynamics*, *66*(5), 637–658. https://doi.org/10.1007/s10236-016-0943-1

Guo, L. C., Brand, M., Sanders, B. F., Foufoula-Georgiou, E., & Stein, E. (2018). Tidal asymmetry and its variability in a short tidal basin with implications on residual sediment transport and basin management. *Advances in Water Resources*, *121*, 1–8.

Guo, L. C., van der Wegen, M., Jay, D. A., Matte, P., Wang, Z. B., Roelvink, J. A., & He, Q. (2015). River-tide dynamics: Exploration of nonstationary and nonlinear tidal behavior in the Yangtze River estuary. *Journal of Geophysical Research: Oceans*, *120*, 3499–3521. https://doi.org/10.1002/2014JC010491

Guo, L. C., van der Wegen, M., Roelvink, J. A., & He, Q. (2014). The role of river flow and tidal asymmetry on 1D estuarine morphodynamics. *Journal of Geophysical Research: Earth Surface*, *119*, 2315–2334. https://doi.org/10.1002/2014JF003110

Guo, L. C., van der Wegen, M., Wang, Z. B., Roelvink, J. A., & He, Q. (2016). Exploring the impacts of multiple tidal constituents and varying river flow on long-term, large scale estuarine morphodynamics by means of a 1D model. *Journal of Geophysical Research: Earth Surface*, *121*, 1000–1022. https://doi.org/10.1002/2016JF003821

Guo, W. Y., Song, D. H., Wang, X. H., Ding, P. X., & Ge, J. Z. (2016). Contributions of different tidal interactions to fortnightly variations in tidal duration asymmetry. *Journal of Geophysical Research: Oceans*, *121*, 5980–5994. https://doi.org/10.1002/2016JC011689

Hoitink, A. J. F., Hoekstra, P., & van Maren, D. S. (2003). Flow asymmetry associated with astronomical tides: Implications for the residual transport of sediment. *Journal of Geophysical Research 108*(C10), 3315–3322. https://doi.org/10.1029/2002JC001539

Jewell, S. A., Walker, D. J., & Fortunato, A. B. (2012). Tidal asymmetry in a coastal lagoon subject to a mixed tidal regime. *Geomorphology*, *138*(1), 171–180. https://doi.org/10.1016/j.geomorph.2011.08.032

Le Provost, C. (1991). Generation of overtides and compound tides (review). In B. B. Parker (Ed.), *Tidal Hydrodynamics* (pp. 269–295). Toronto: John Wiley.

LeBlond, P. H. (1991). Tides and their interactions with other oceanographic phenomena in shallow water (review). In B. B. Parker (Ed.), *Tidal Hydrodynamics* (pp. 357–378). Toronto: John Willey.

Lincoln, J. M., & Fitzgerald, D. M. (1988). Tidal distortion and flood dominance at five small tidal inlets in southern Maine. *Marine Geology*, *82*(3-4), 133–148. https://doi.org/10.1016/0025-3227(88)90137-5

Matte, P., Jay, D. A., & Zaron, E. D. (2013). Adaptation of classical tidal harmonic analysis to nonstationary tides, with application to river tides. *Journal of Atmospheric and Oceanic Technology*, *30*(3), 569–589. https://doi.org/10.1175/JTECH-D-12-00016.1

Nidzieko, N. J. (2010). Tidal asymmetry in estuaries with mixed semidiurnal/diurnal tides. *Journal of Geophysical Research*, *115*, C08006. https://doi.org/10.1029/2009JC005864

Pawlowicz, R., Beardsley, B., & Lentz, S. (2002). Classical tidal harmonic analysis including error estimates in MATLAB using T_TIDE. *Computers & Geosciences*, *28*(8), 929–937. https://doi.org/10.1016/S0098-3004(02)00013-4

Postma, H. (1961). Transport and accumulation of suspended matter in the Dutch Wadden Sea. *Netherlands Journal of Sea Research*, *1*(1-2), 148–190. https://doi.org/10.1016/0077-7579(61)90004-7

Pugh, D. T. (1987). *Tides, surges and mean sea-level* (486 pp.). New York: John Wiley.

Ranasinghe, R., & Pattiaratchi, C. (2000). Tidal inlet velocity asymmetry in diurnal regimes. *Continental Shelf Research*, *20*(17), 2347–2366. https://doi.org/10.1016/S0278-4343(99)00064-3

Reichman, B. O., Muhlestein, M. B., Gee, K. L., Neilson, T. B., & Thomas, D. C. (2016). Evolution of the derivative skewness for nonlinearly propagating waves. *The Journal of the Acoustical Society of America*, *139*(3), 1390–1403. https://doi.org/10.1121/1.4944036

van Rijn, L. C. (1993). *Principles of sediment transport in rivers, estuaries and coastal seas*. Aqua Publications, The Netherlands.

Ruessink, B. G., van den Berg, T. J. J., van Rijn, L. C. (2009). Modeling sediment transport beneath skewed asymmetric wave above a plane bed. *Journal of Geophysical Research 114*, C11021. https://doi.org/10.1029/2009JC005416

Sassi, M. G., & Hoitink, A. J. F. (2013). River flow controls on tides and tide-mean water level profiles in a tidal freshwater river. *Journal of Geophysical Research: Ocean*, *118*, 4139–4151. https://doi.org/10.1002/jgrc.20297

Shepherd, M. R., Gee, K. L., & Hanford, A. D. (2011). Evolution of statistical properties for a nonlinearly propagating sinusoid. *The Journal of the Acoustical Society of America*, *130*(1), EL8–EL13. https://doi.org/10.1121/1.3595743

Song, D. H., Wang, X. H., Kiss, A. E., & Bao, X. W. (2011). The contribution of tidal asymmetry by different combinations of tidal constituents. *Journal of Geophysical Research*, *116*, C12007. https://doi.org/10.1029/2011JC007270

Speer, P. E., & Aubrey, D. G. (1985). A study of non-linear tidal propagation in shallow inlet/estuarine systems. Part II: Theory. *Estuarine, Coastal and Shelf Science*, *21*(2), 207–224. https://doi.org/10.1016/0272-7714(85)90097-6

van de Kreeke, J., & Robaczewska, K. (1993). Tide-induced residual transport of coarse sediment: Application to the ems estuary. *Netherlands Journal of Sea Research*, *31*(3), 209–220. https://doi.org/10.1016/0077-7579(93)90022-K

Wang, Z. B., Jeuken, C., Gerritsen, H., de Vriend, H. J., & Kornman, B. A. (2002). Morphology and asymmetry of the vertical tide in the Westerschelde estuary. *Continental Shelf Research*, *22*(17), 2599–2609. https://doi.org/10.1016/S0278-4343(02)00134-6

Wang, Z. B., Juken, H., & de Vriend, H. J. (1999). Tidal asymmetry and residual sediment transport in estuaries. WL|Hydraulic, report No. Z2749, 66 pp.

Zhang, M., Townend, I., Zhou, Y. X., & Cai, H. Y. (2016). Seasonal variation of river and tide energy in the Yangtze estuary, China. *Earth Surface Processes and Landforms*, *41*(1), 98–116. https://doi.org/10.1002/esp.3790

Zhou, Z., Coco, G., Townend, I., Gong, Z., Wang, Z. B., & Zhang, C. K. (2018). On the stability relationships between tidal asymmetry and morphologies of tidal basins and estuaries. *Earth Surface Processes and Landforms*, *43*, 1943–1959. https://doi.org/10.1002/esp.4366